Diffusion tensor magnetic resonance tractography of the prostate: feasibility for mapping neurovascular anatomy

Daniel Jason Aaron Margolis[1], Benjamin Ellingson[2], Shyam Natarajan[3], Robert Reiter[4], Taryar Zaw[1], Peter Schulam[4], Steven Raman[1], and David Finley[5]

[1]Department of Radiology, UCLA David Geffen School of Medicine, Los Angeles, CA, United States, [2]Department of Radioloyg, UCLA David Geffen School of Medicine, [3]Department of Bioengineering, UCLA David Geffen School of Medicine, Los Angeles, CA, United States, [4]Department of Urology, UCLA David Geffen School of Medicine, [5]Department of Urology, Kaiser Permanente Los Angeles

Introduction

Definitive treatment of prostate cancer involves either surgery or radiation therapy. Although advances in both have reduced the incidence of side effects, injury to the nerves that run alongside the prostate can result in debilitating incontinence and impotence. Identification of the neurovascular bundle is difficult even with optical magnification. This study looks at the potential of diffusion tensor imaging as a potential solution.

Methods

Following Institutional Review Board approval, eight patients underwent multiparametric endorectal MRI of the prostate on a 3.0 Tesla MR scanner including T2-weighted imaging (TSE, TR 3800-5040 TE 101 ms, ETL 13, 3 mm, no gap, matrix 256 x 205, 14 x 14 cm FOV) and diffusion tensor imaging using a twice-refocused echo-planar acquisition, 12 non-colinear diffusion sensitizing directions, and and b values of 0 and 600 $^{mm}/s^2$. DTI tractography image processing was performed using the Diffusion Toolkit version 0.6.1 and TrackVis version 0.5.1 (Ruopeng Wang, Van J. Wedeen, TrackVis.org, Martinos Center for Biomedical Imaging, Massachusetts General Hospital). Spherical regions of interest (ROIs) with a radius of 1.5mm (volume – 14.14 mm3) were used for evaluation of fiber tracts (e.g. tract number, tract density) within the periprostatic space, based on evaluation of anatomic T2 images and whole-mount prostatectomy specimens. Fiber tracts were constructed for each patient using an angle threshold of 35° and a Tensorline propagation algorithm with bootstrapping from multiple directions and averages. ROIs were placed at standardized regions of the prostate: prostatic apex (6mm cephalad to the urethra), mid-gland (median prostate slice number), and prostate base (6mm caudad to the bladder). The per-voxel absolute vector values were color-coded: red (medio-lateral direction), blue (cranio-caudal direction) and green (anterior-posterior direction).

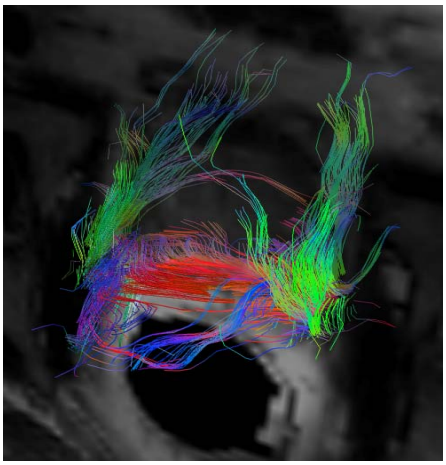

Figure 1: DTI tractography images of the neurovascular bundles in a single patient. *Selective ROIs were used to visualize neurovascular bundles in side-to-side interconnections (red), vertical communicating fibers (green), and "classic" parallel fibers (blue).*

Results

A lush network of tract fibers was identified around the entire border of the prostate in the region between the prostatic capsule and lateral prostatic fascia. While the majority of fiber tracts were found running parallel to the prostatic surface, a number of fibers were also identified travelling horizontally and vertically. A wide degree of variation was observed in total tract number (range: 709-2855, SD=875) between patients and regions of the prostate. The total tract mass, corrected for prostate volume (normalized tract number = tract # / ROIs), was significantly larger for the lower prostate hemisphere compared with the upper hemisphere at the base of the prostate. At the mid prostate, there was no significant difference in fiber mass between the upper and lower hemispheres. At the prostatic apex, the upper hemisphere contained the significantly more fiber mass than the lower hemisphere. The postero-lateral sectors, representing the putative "classic" region of the dominant NVB, accounted for approximately 32.3% of the total tract mass. The postero-lateral tracts on the right and left side of the prostate were connected by a broad commissure-like plexus of fibers posteriorly in the region of Denonvillier's fascia. The degree of crossover varied significantly between patients.

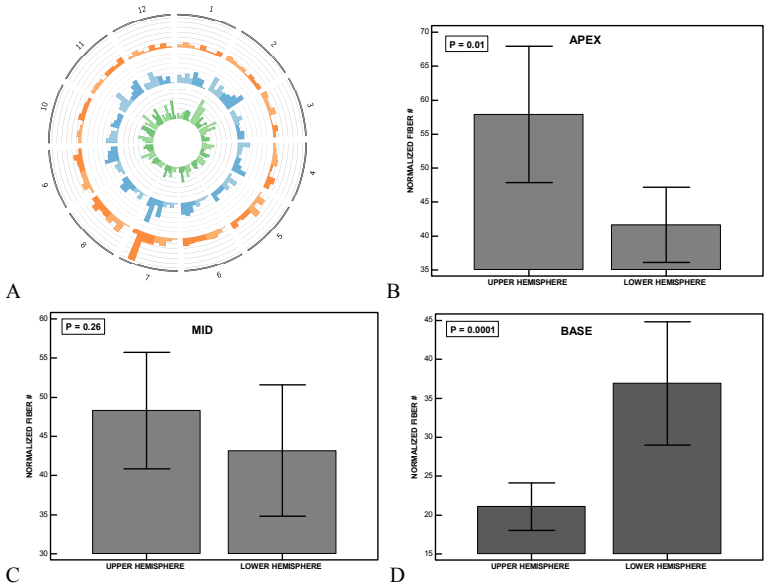

Figure 2: Fiber Tract Density by Region. *A) Circular ideogram showing sector-based histograms of tract density (fibers / mm) at the base (orange), mid (blue) and apex (green). B) Fiber tract density in the apex. C) Fiber tract density in the mid region. D) Fiber tract density in the base region.*

Discussion

Although promising as a technique to guide surgery and radiation therapy, this proof-of-concept study raises as many questions as it answers, with preliminary findings suggesting a more complex anatomy than has been previously appreciated. Although DTI is undoubtedly capturing some non-nerve fiber tracts (e.g. blood vessels) that run within the periprostatic space, it is probable that much of the fiber-tract mass that we visualized represents nerve fibers.

References

Ellingson BM, et al. Diffusion tensor magnetic resonance imaging in spinal cord injury. Concepts in Mag Res Part A 2008; 32A: 219-237.

Lazar M, et al: Bootstrap analysis of DT-MRI tractography techniques: steamlines and tensorlines. Proc Intl Soc Mag Reson Med 2001; 9:1527